Damage simulation of fracture asperity in geothermal systems

Chao Zeng*[1], Wen Deng[1], Yiming Jin[1]

[1] Department of Civil, Architectural, and Environmental Engineering, Missouri University of Science and Technology

*Corresponding author: 211 Butler-Carlton Hall, 1401 N. Pine St., Rolla, MO 65409. zc727@mst.edu

Abstract: Thermal-mechanical analysis of rock is analyzed by isotropic damage mechanics. The simulation is implemented by equation-based modelling interface and Heat Transfer in Solids interface. The mechanical analysis is carried out in Weak Form PDE interface in combination with Domain ODE interface and Helmholtz Equation interface. The historical dependent damage variable is specially treated by Previous Solution solver to ensure monotonic increasing property. The cooling induces significant thermal strain and correspondingly affects damage variable. This process is split into three steps in simulation: initial displacement loading of asperity, constant stress loading of asperity, thermal cooling of asperity. The evolution of damage is captured in each stage to analyze the degradation of asperity in geothermal systems.

Keywords: fracture asperity, damage mechanics. Thermal effect, geothermal systems

1. Introduction

Fracture as a major factor which greatly affects the fluid flow, heat recovery in subsurface. Natural fractures are usually maintained by asperity self-propping (The size of asperity varies from tens of nanometers to several millimeters). The in-situ stress loading on fractures are balanced by contacting asperity pairs. In some engineering projects, e.g., enhanced geothermal systems, the cold water is pumped into deep formation (usually larger than 3km) and then transfers heat with in-situ hot rock in natural fractures. The significant temperature difference between the invading fluid and hot asperity induces the asperity stress change and the shrinkage of contact asperity [1]. At the same time, the overburden pressure loading on asperity remains the same. Hence, the vertical compression of asperity could take place under the effect of thermal shrinkage. This compression gives rise to damage of asperity pairs and reduces fracture aperture significantly.

In this paper, an isotropic scalar damage constitutive law is implemented in COMSOL Multiphysics® and combined with Heat Transfer in Solids interface. The initial loading state of fracture asperity is implemented by Weak Form PDE interface without temperature effects. Then the cooling of asperity surface and stress evolution in asperity are simulated by segregated solver.

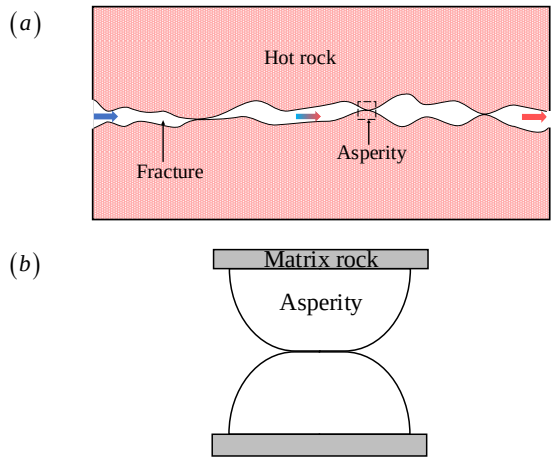

Figure 1. (a) Cold fluid flows through fracture with hot matrix rock [2], (b) asperity model to be simulated in this study.

2. Governing equations

2.1 Isotropic damage mechanics

The model here implemented is an extension of the Solid mechanics interface in COMSOL Multiphysics® which is based on the standard momentum balance equation. For simplicity, inertial effects are here neglected, and displacements and strains assumed to remain small. This leads to the following governing equations:

$$\nabla \cdot \boldsymbol{\sigma} + \boldsymbol{F}_v = 0 \tag{1}$$

$$\boldsymbol{\varepsilon} = \frac{1}{2}\left(\nabla \boldsymbol{u} + \nabla \boldsymbol{u}^T\right) \tag{2}$$

In Eq. (1), $\boldsymbol{\sigma}$ is the stress tensor and $\boldsymbol{F}_v$ indicates the body forces, while in Eq. (2), $\boldsymbol{\varepsilon}$ is the total strain tensor and $\boldsymbol{u}$ are the displacements. These two equations are then complemented by appropriate boundary conditions and a constitutive law relating stress and strains to complete the problem definition.

In description of local deformation of brittle material, e.g., concrete and rock, a popular class of constitutive law are based on continuum damage mechanics (CDM) [3]. CDM is a constitutive theory that describes the progressive loss of material integrity due to the propagation and coalescence of microcracks, micro-voids, and similar defects. These changes in the microstructure lead to a degradation of material stiffness observed on the macroscale. The simplest damage theory is achieved by the isotropic damage model with a single scalar variable. Isotropic damage models are based on the simplifying assumption that the stiffness degradation is isotropic, i.e., stiffness moduli corresponding to different directions decrease proportionally, independently of the direction of loading [4]. Correspondingly, the damaged stiffness tensor is expressed as

$$\mathbf{C}_{\boldsymbol{d}} = (1-D)\mathbf{C} \tag{3}$$

Where $\mathbf{C}$ is the elastic stiffness tensor of the intact material, $\mathbf{C}_\mathbf{d}$ is the elastic stiffness tensor of damage material, and D is the scalar damage variable. In the present context, $\mathbf{E}_\mathbf{s}$ is the secant stiffness that relates the total strain to total stress, according to the formula

$$\boldsymbol{\sigma} = \mathbf{C}_\mathbf{d} : \boldsymbol{\varepsilon}_{\boldsymbol{e}} = (1-D)\mathbf{C} : \boldsymbol{\varepsilon}_{\boldsymbol{e}} \tag{4}$$

Where $\boldsymbol{\sigma}$ is nominal stress tensor, also used in Eq. (1), $\boldsymbol{\varepsilon}_{\boldsymbol{e}}$ is the elastic strain tensor. The effective stress tensor is defined as

$$\bar{\boldsymbol{\sigma}} = \mathbf{C} : \boldsymbol{\varepsilon}_{\boldsymbol{e}} \tag{5}$$

The local response on the microscopic scale follows the Eq. (3)-(5). The macroscopic response of material under loading represents non-linear property and controlled by the evolution of damage variable D. A loading function f is introduced to specify the elastic domain and the states at which damage grows.

$$f(\boldsymbol{\varepsilon}, \kappa) = \tilde{\varepsilon}(\boldsymbol{\varepsilon}) - \kappa \tag{6}$$

The loading function depends on the strain tensor $\boldsymbol{\varepsilon}$ and on a variable κ that controls the evolution of the elastic domain. Physically, κ is the largest strain level ever researched in the history of the material. Like plasticity theory, $f(\boldsymbol{\varepsilon}, \kappa) < 0$ are in the elastic domain. Damage grows only if $f(\boldsymbol{\varepsilon}, \kappa) = 0$. In Eq. (6), $\tilde{\varepsilon}$ is the equivalent strain, a scalar measure of the strain level. The definition of equivalent strain determines the shape of the elastic domain. For rock and concrete with very different behaviors in tension and in compression. Microcracks grow mainly if the material is stretched, and so it is natural to consider only normal strains that are positive and neglect those that are negative. Mazars definition of equivalent strain is used in this study [5]

$$\tilde{\varepsilon} = \left\| \langle \boldsymbol{\varepsilon} \rangle \right\| = \sqrt{\langle \boldsymbol{\varepsilon} \rangle : \langle \boldsymbol{\varepsilon} \rangle} \tag{7}$$

Where McAuley brackets $\langle \cdot \rangle$ denote the "positive part" operator. After the spectral decomposition of strain tensor combined with "positive part" operator, the equivalent strain can be rewritten as

$$\tilde{\varepsilon} = \sqrt{\sum_{I=1}^{3} \langle \varepsilon_I \rangle^2} \tag{8}$$

Where $\varepsilon_i \, (i = 1,2,3)$ is the principal strain component. The evolution of elastic domain is controlled by a set of loading/unloading conditions on the Karush-Kuhn-Tucker condition

$$f \le 0, \ \dot{\kappa} \ge 0, \ \dot{\kappa} f = 0 \tag{9}$$

The evolution of damage variable D is also necessary to complement the loading/unloading damage process. At here, the damage function can be defined as

$$D_t(\kappa) = 1 - (1 - A_t)\frac{\varepsilon_0}{\kappa} - A_t \exp\left[-B_t(\kappa - \varepsilon_0)\right] \tag{10}$$

$$D_c(\kappa) = 1 - (1 - A_c)\frac{\varepsilon_0}{\kappa} - A_c \exp\left[-B_c(\kappa - \varepsilon_0)\right] \tag{11}$$

Where D_t and D_c are damage variables in tension and compression respectively. ε_0 is the damage threshold. A_t, B_t, A_c and B_c are constant parameters controlling the shape of damage function curve.

When considering both tensile and compressive damage, a general value of D is obtained as a linear combination

$$D = \alpha_t D_t + \alpha_c D_c \tag{12}$$

Where the coefficients α_t and α_c take into account the character of the stress state.

$$\alpha_t = \sum_{I=1}^{3} \frac{\varepsilon_{tI} \left\langle \varepsilon_I \right\rangle}{\tilde{\varepsilon}^2} \tag{13}$$

$$\alpha_c = 1 - \sum_{I=1}^{3} \frac{\varepsilon_{tI} \left\langle \varepsilon_I \right\rangle}{\tilde{\varepsilon}^2} \tag{14}$$

The failure envelope of Mazars model is not realistic in the region of compression. A partial improvement is obtained if the equivalent strain is adjusted by the multiplicative factor

$$\gamma = \frac{\sqrt{\sum_{I=1}^{3} \left\langle \sigma_I^- \right\rangle^2}}{\sum_{I=1}^{3} \left| \sigma_I^- \right|} \tag{15}$$

Where $\sigma_I^- = -\left\langle -\sigma_I \right\rangle$ are the negative parts of principal stresses. The adjustment is done only if at least two principal stresses are negative and none of them is positive.

2.2 Heat conduction

The temperature distribution $T(x,y)$ in asperity by cooling is obtained by heat conduction equation. Considering the instant propagation of heat and small size of fracture asperity, stationary heat conduction is solved

$$\alpha_{th} \nabla^2 T = 0 \tag{16}$$

Where α_{th} is thermal diffusivity of designated material.

2.3 Thermal expansion

The cooling of surface would induce thermal strain in material. The thermal strain is calculated by

$$\boldsymbol{\varepsilon_{th}} = \boldsymbol{\alpha}\left(T - T_{ref}\right) \tag{17}$$

Where $\boldsymbol{\alpha}$ is the coefficient of thermal expansion tensor. In this study, $\boldsymbol{\alpha}$ is a diagonal matrix with same value under the assumption of isotropic material.

If thermal strain is the only inelastic strain considered, the elastic strain in Eq. (4)-(5) can be defined

$$\boldsymbol{\varepsilon_e} = \boldsymbol{\varepsilon} - \boldsymbol{\varepsilon_{th}} \tag{18}$$

3. Numerical consideration

The isotropic damage model in section 2.1 has strong mesh dependency of the results. In this way, the results would be objective, meaning that the results do not converge to a single solution upon mesh refinement. To overcome this deficiency in finite element framework, two possible approaches are often mentioned [6]: 1. Use a stress-strain law that at each material point depends on the element size, 2. Add a localization limiter to the constitutive law so that the simulated localization zone corresponds to that observed experimentally. The implementation of these two approaches are referred to Gasch's work [6].

In this study, the local cracking direction or crack band width is not the point of interest. Therefore, non-local model is used to alleviate mesh dependency. A localization limiter enforces a realistic and mesh-independent size of strain softening region by supplying more information about the material structure to the constitutive law. A higher-order deformation gradient in the constitutive model is introduced to remedy the deficiency of mesh dependency [7]. The expression in Eq. (7) or (8) is the local equivalent strain in a certain material point. The localized deformation in quasi-brittle would induce discontinuous strain. The non-local equivalent strain in a material point is a weighted average of the local equivalent strain over the surrounding volume. The non-local equivalent strain $\overline{\varepsilon}$ satisfy gradient damage formulation

$$\overline{\varepsilon} - c\nabla^2 \overline{\varepsilon} = \tilde{\varepsilon} \tag{19}$$

Where gradient parameter c is of the dimension length squared, so that an internal length scale is present in the gradient formulation. Eq. (19) is complemented with natural boundary condition

$$\nabla \overline{\varepsilon} \cdot \boldsymbol{n} = 0 \tag{20}$$

4. Implementation in COMSOL Multiphysics®

The implementation in COMSOL Multiphysics® is done by Heat Transfer in Soilds interface and equation-based modeling. The heat transfer in solids interface is used to obtain temperature distribution in the asperity. Then it's invoked by weak form PDE interface to calculate thermal strain. Weak form PDE interface is used to implement isotropic damage model. The internal variables in stress analysis, i.e., stress and strain components, are defined in variable definition node. Then weak form of linear elastic material is derived and input into the interface. The variable κ needs special consideration. Because it characterizes the non-linear and history dependent response of the damage model. Based on Eq. (9), κ is

monotonically increasing. A Domain ODE and DAEs interface is set up to calculate κ_0 to ensure that κ_0 is the maximum strain in previous calculation step. Previous Solution solver is needed to store value of κ_0 in last calculation step. In addition, the gradient formation is implemented by Helmholtz Equation interface with zero flux boundary condition to calculate non-local equivalent strain $\bar{\varepsilon}$ in current calculation step. Then, the internal variable κ is the maximum of κ_0 and $\bar{\varepsilon}$. That is, current k is maximum value in previous maximum strain κ_0 and current non-local equivalent strain $\bar{\varepsilon}$.

The geometry used in simulation is shown in Fig. 2. Based on the involved physics introduced in section 1, displacement and temperature boundary condition are set up respectively. For the displacement boundary setting, the bottom boundary condition is roller associated with zero horizontal movement in middle point, to release shrinkage in horizontal direction. The left and right sides boundary condition is natural boundary condition. The top boundary condition is stress boundary condition to simulate the in-situ stress loading on the asperity. For the temperature boundary setting, the boundary is thermal insulation, on the assumption that two contacting asperities has no heat flux in contact region. It's reasonable for same size of contacting asperities. The top boundary is Dirichlet temperature condition with T_{init}. The left and right sides boundary condition is Dirichlet temperature condition with T_{water}.

The mesh info is also shown in Fig. 2. The total number of mesh is 3630. The minimum mesh size is 0.026 mm, residing the two corners of bottom boundary. When the top surface is loaded, the two sharp corners would have stress singularity. To reduce this artificial effect, fillet tool is applied in the geometry construction.

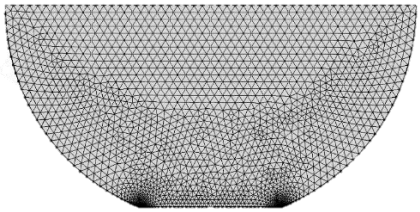

Figure 2. meshed asperity model used in simulation.

5. Simulation results

5.1 Mechanical analysis

Before the injection of cold water, the fracture asperity is subject to in-situ stress. Hence, the initial state of asperity is analyzed first to get insight in the initial deformation of asperity and damage state.

The stress loading on top of asperity is not equivalent to in-situ stress. There's the mapping relation between in-situ stress and stress on asperity: [8]

$$\sigma = \frac{\sigma_v - 2.46P_p}{0.54} \tag{21}$$

Where P_p is the pore pressure at the depth of the asperity, σ_v is the in-situ tectonic stress, and σ is the effective stress on the asperity.

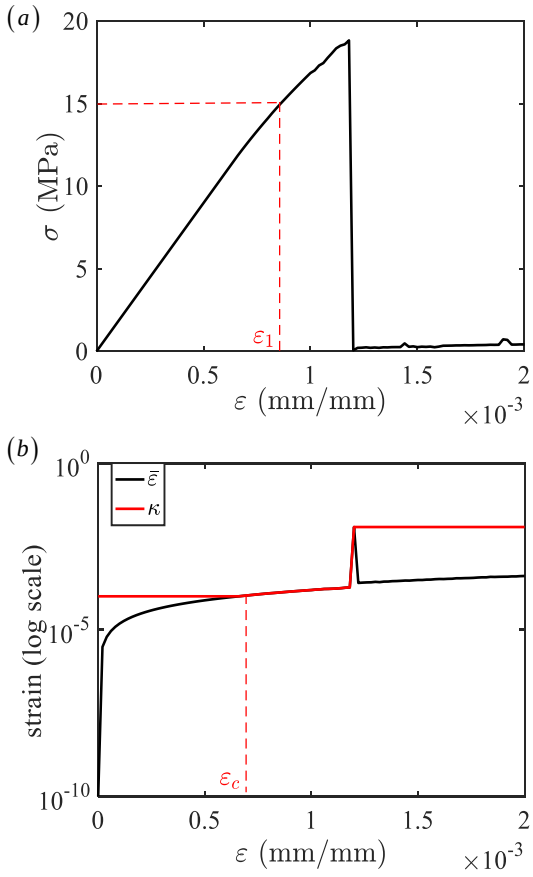

Figure 3. (a) Stress and strain correlation with displacement loading condition, and (b) corresponding internal variable κ and non-local equivalent strain. $\varepsilon_1 = 0.86\times10^{-3}$ is the strain corresponding to $\sigma = 15MPa$ as initial condition for thermal-mechanical analysis. $\varepsilon_c = 0.66\times10^{-3}$ is the start point of nonlinear stage.

In Fig. 3a, stress drop abruptly at strain 1.2×10^{-3}. After that point, asperity loss bearing

capacity and most elements are damaged. Before that point, two segments can be observed but not noticeable. The first segment is linear stage and the second segment is hardening stage. The bounding line is not noticeable. But it can be inferred from Fig. 3b. the damage threshold ε_0 is 0.1×10^{-3}, which means no damage if κ is equal to ε_0. The initiation point of damage is $\varepsilon_c = 0.66 \times 10^{-3}$. With vertical strain ε larger than ε_c, κ increase monotonically. After most elements are damaged, κ asymptotically reaches to a historical maximum, 0.012.

The geothermal systems are in the 3km ~5km. The corresponding loading stress on asperity is in the range of 2MPa ~ 7.5MPa based on the mapping expression Eq. (21). Notice that the stress calculated from Eq. (21) is for semi-spherical asperity. For the plane stress condition in this simulation with unit thickness in the third direction., the loading stress corresponding to 4 MPa in circular contact is approximately 15 MPa Therefore, the stress and strain in the initial condition are 15MPa and 0.86×10^{-3} respectively. The damage contour of initial condition is presented in Fig. 4.

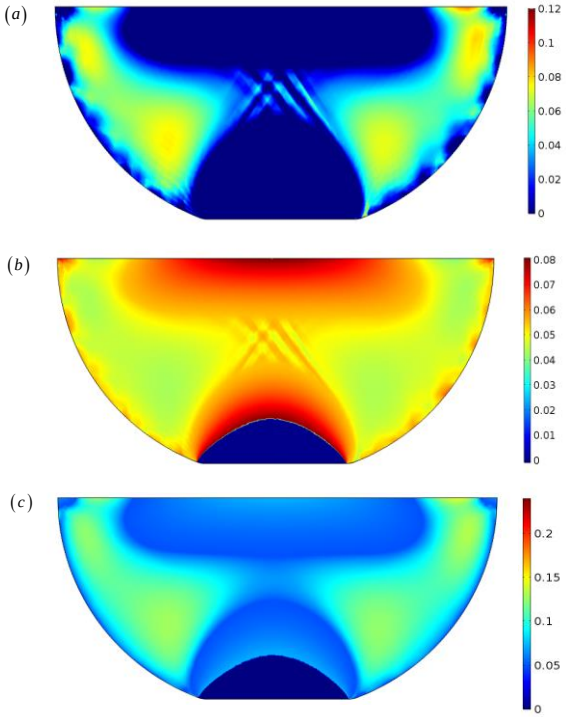

Figure 4. (a) Tensile damage variable $\alpha_t D_t$ at $\sigma = 15MPa$, (b) compressive variable $\alpha_c D_c$ at $\sigma = 15MPa$, and (c) total damage variable D at $\sigma = 15MPa$.

The tensile, compressive and total damage contour is displayed. At this stress condition, stiffness most element away from the boundary condition degraded a little. The tensile and compressive degradation dominates different regions. Tensile damage occurs near the circular surface of geometry, whereas compressive damage is centered on vertical direction aligned with the symmetric axis. This distinct distribution of tensile and compressive damage has significant effects on the thermal damage in following section.

5.2 Thermal-mechanical analysis

When cold water is pumped into the fracture, the high temperature difference between water temperature T_{water} and initial hot rock temperature T_{init} would induce significant thermal strain. While the top of asperity is subjected to constant loading stress, the damage of asperity would induce vertical crushing of asperity.

Heat Transfer in Solids interface is run first to obtain the temperature distribution within the asperity. The boundary setting for temperature is mentioned in section 4. The stationary temperature distribution is shown in Fig.5.

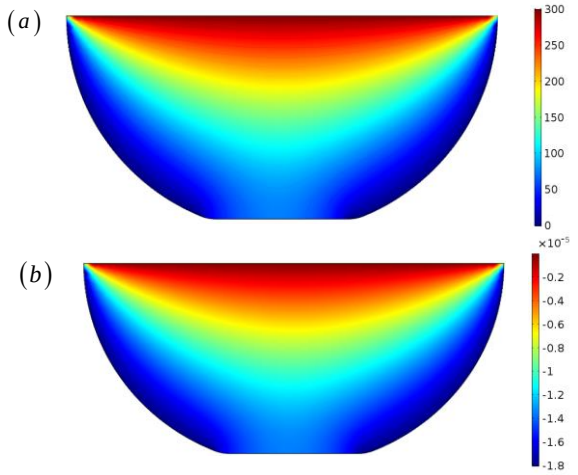

Figure 5. (a) Temperature distribution within asperity at steady state, (b) induced thermal strain distribution. The temperature difference in this display is at maximum, 300℃.

The solution from former section is input into new stationary solver as initial value. For this stationary study, water temperature T_{water} is ramped from 0°C to 300°C, corresponding to different distances to injection well. Because, the water is heated up gradually along flow direction. The display of maximum temperature difference is in Fig. 5. The

stress and damage variation for different temperature difference ($\Delta T = T_{init} - T_{water}$) is presented in Fig. 6.

Two stage of compression can be observed in Fig. 6a. The first stage has higher strain gradient than the second stage. The border point is $\Delta T_c = 48°C$. In combination with Fig. 6b, damage takes place in both stages, inferring from increasing internal variable κ. The rapid increase of internal variable before $\Delta T_c = 48°C$ indicates more elements are degraded in first stage than that in second stage.

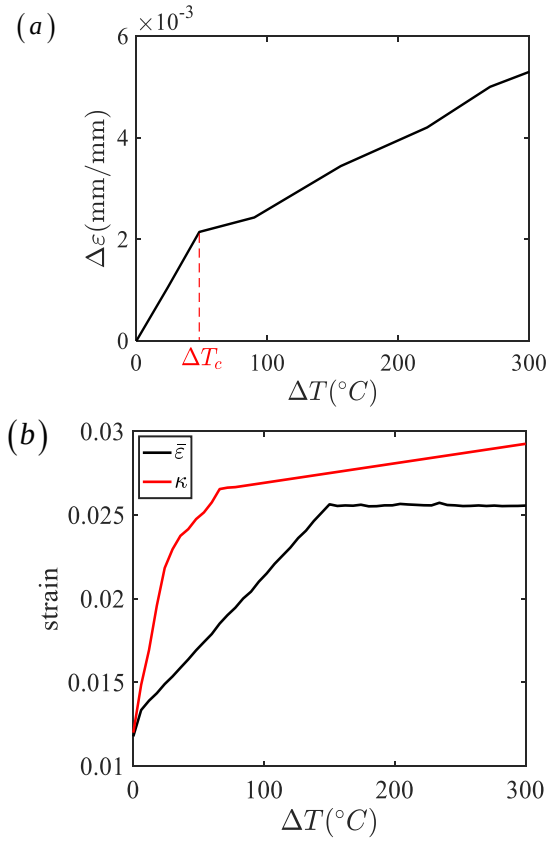

Figure 6. (a) The vertical compression with response to temperature difference, (b) the internal variable κ and non-local equivalent strain $\bar{\varepsilon}$ variation with temperature difference.

The damage contour (Fig. 7) for thermal-mechanical analysis is also presented to visualize the underlying mechanism of vertical deformation in Fig. 6a. From Fig. 7b, damaged elements present in the corner of contact. This is the cracking initiation point. As temperature difference increases, crack propagates along radial direction. The circular low damage region new the bottom boundary is due to boundary setting. To improve the accuracy of this simulation, reasonable contact boundary should be set to analyze the effect of contact pressure on the asperity damage.

The radial cracking in Fig. 7 is due to radial shrinkage induced by boundary cooling. In Fig. 5b, highest strain gradient is near the top corner of asperity, since the horizontal displacement of top boundary is constrained. The first principal strain at initiation point is shown in Fig. 8. The maximum first principal strain is at the corner to induce tensile damage of elements.

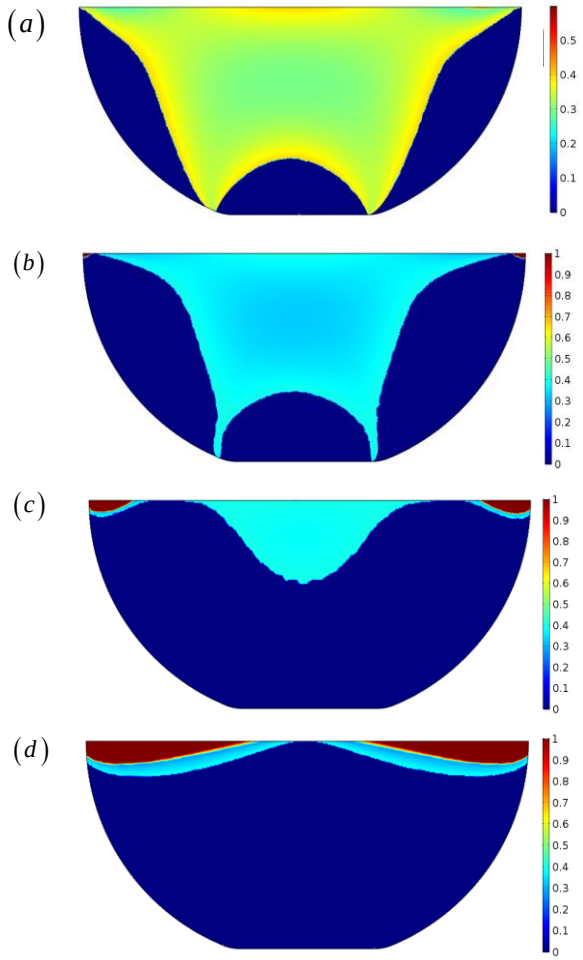

Figure 7. Damage variable D contour at (a) $\Delta T = 24°C$, (b) $\Delta T = 48°C$, (c) $\Delta T = 100°C$ and (d) $\Delta T = 300°C$.

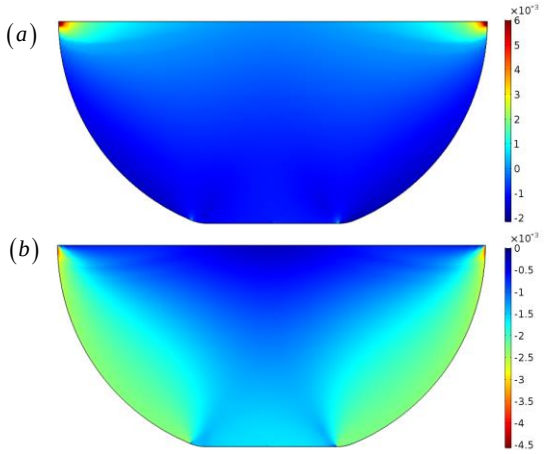

Figure 8. First principal strain and second principal strain distribution at $\Delta T = 48°C$.

The value of variable used in this simulation is listed in Table 1.

Table 1. The variable used in the model

Variable	Value	Units
R	2.5	mm
E	30	MPa
ν	0.2	1
α	6×10^{-8}	1/℃
ρ	2600	kg/m^3
A_t	0.81	1
B_t	10450	1
A_c	1.34	1
B_c	2537	1
ε_0	1×10^{-4}	1
T_{init}	350	°C
T_{water}	50	°C

6. Conclusion

A Thermal-mechanical model of rock is presented to analyze the potential damage of fracture asperity in geothermal systems. Isotropic damage model has been used to characterize the damage of rock. The thermal expansion is incorporated into the damage model in the cooling of rock. Two analysis have been conducted based on this model. The mechanical deformation of asperity under displacement loading condition and thermal-mechanical deformation of asperity under stress control condition. It shows that asperity is already degraded in the high stress condition. When cooled by cold water, significant thermal strain induces radial cracking on the top corner of asperity and decrease its loading capacity significantly.

Several improvements will be done to increase accuracy of this simulation. More realistic three-dimensional model will be considered. In addition, contact pair setting is necessary to accurately track the deformation at the contact region, other than far from contact region. Damage variable and temperature can be fully coupled in those governing equations.

7. Reference

1. Zeng C., Deng W., Wu C., Insall M. Thermal stress effect on fracture integrity in enhanced geothermal systems. *Proceedings of GeoShanghai 2018* International Conference: Rock Mechanics and Rock Engineering. GSIC 2018, 388-96 (2018).
2. Zeng, C., Deng, W. The effect of radial cracking on the integrity of asperity under thermal cooling Process. *American Rock Mechanics Association*, 2018.
3. Lemaitre, Jean, and Rodrigue Desmorat. Engineering damage mechanics: ductile, creep, fatigue and brittle failures. Springer Science & Business Media, 2005.
4. Jirásek, Milan. "Damage and smeared crack models." *In Numerical modeling of concrete cracking*, pp. 1-49. Springer, Vienna, 2011.
5. J Mazars and G Pijaudier-Cabot, Continuum Damage Theory —Application to Concrete, *Journal of Engineering Mechanics*, 115, 345-65 (1989)
6. Gasch, Tobias, and Anders Ansell. Cracking in quasi-brittle materials using isotropic damage mechanics. In *Proceedings, Comsol Conference*. 2016.
7. Peerlings, RHJ D., R. De Borst, WAM D. Brekelmans, and J. H. P. De Vree. Gradient enhanced damage for quasi-brittle materials. *International Journal for numerical methods in engineering* 39, no. 19 (1996): 3391-3403.
8. Zeng C., Deng W., Wu C. Thermal effect of cold fluid injection on fracture integrity of hot dry rock and its implication of heat production efficiency of enhanced geothermal systems. *Geothermics*, 2018. (In review)